



PERGAMON

Available online at www.sciencedirect.com

SCIENCE @ DIRECT®

Electrochimica Acta 49 (2003) 73–83

ELECTROCHIMICA
Actawww.elsevier.com/locate/electacta

The adsorption of Sn on Pt(1 1 1) and its influence on CO adsorption as studied by XPS and FTIR

S. Tillmann^a, G. Samjeské^a, K.A. Friedrich^{b,1}, H. Baltruschat^{a,*}^a *Institut für Physikalische und Theoretische Chemie, Universität Bonn, Römerstraße 164, D-53117 Bonn, Germany*^b *Physik Department E19, Technische Universität München, James-Frank Str. 1, D-85748 Garching, Germany*

Received 28 January 2003; accepted 11 July 2003

Abstract

The coverage of Sn on Pt(1 1 1) which is obtained by electrochemical deposition from 5×10^{-5} M Sn^{2+} in 0.5 M H_2SO_4 has been determined by XPS for different deposition times. Complete suppression of hydrogen adsorption corresponds to a coverage of $\vartheta_{\text{max}} = 0.35$ (Sn to surface Pt atoms).

Co-adsorption of CO with Sn on Pt(1 1 1) has been studied by FTIR spectroscopy. The IR spectra of the stretching vibration of CO can be interpreted in terms of the vibrational signature of the Pt(1 1 1)/CO system and no vibrational bands associated with CO on Sn are detected. At high Sn coverages, the 1840 cm^{-1} band associated with bridge-bonded CO and the 2070 cm^{-1} band assigned to on-top CO are present, however, no hollow site adsorption which is characterized by the 1780 cm^{-1} band is revealed within the resolution of the experiment. This vibrational signature corresponds to a less compressed adlayer compared to the (2×2) -3CO saturation structure on Pt(1 1 1). At lower Sn coverages, signatures from both the compressed and the less compressed CO adlayer structures are seen in the spectra. From earlier structural and electrochemical studies it is known that Sn is adsorbed in 2D islands and influences CO molecules in its neighbourhood electronically. This leads to a disappearance of the IR band from CO adsorbed in the hollow site at high Sn coverages and to higher population of the weakly adsorbed state of CO for all Sn-modified surfaces, i.e. a relative increase of the amount of CO oxidised at low potentials. In addition to this electronic effect, Sn also exerts a co-catalytic effect at low Sn coverages on that part of CO which is adsorbed at a larger distance from Sn due to a bi-functional mechanism. The IR spectra shows for the Sn-modified Pt(1 1 1) surface that the transition from the compressed CO adlayer which is characterized by the hollow site adsorption of CO to the less compressed one which exhibits a characteristic band associated with bridge-bonded CO occurs already at 250 mV instead of 400 mV.

© 2003 Elsevier Ltd. All rights reserved.

Keywords: CO adsorption; CO oxidation; Sn adsorption; Pt(111); IR spectroscopy; XPS; FTIR

1. Introduction

Despite its importance for low temperature fuel cells, the exact mechanism of CO oxidation on Pt and the role of co-catalysts is still far from being understood. On Pt(1 1 1), the saturation coverage of CO corresponds to a (2×2) -3CO adlayer with the coverage of $\vartheta = 0.75$ at low potentials according to STM and FTIR results [1]. Here, the coverage ϑ is the ratio of CO molecules to Pt-surface atoms. At a potential around 0.4 V a part of the adsorbate is oxidised, and the adlayer transforms into a lower coverage adlayer with $\vartheta = 0.68$; Villegas et al. have suggested a $(\sqrt{19} \times \sqrt{19})R$

23.4° structure based on STM results [1]. It is generally accepted that the oxidation of the adlayer proceeds according to a Langmuir–Hinshelwood mechanism. The exact identity of the oxygen species, however, is not really clear. Also, there are contradictory results described in the literature concerning the surface diffusion of CO. Whereas, fast diffusion should lead to the classical rate equation for a Langmuir–Hinshelwood mechanism usually treated in textbooks (the rate is proportional to $\Theta(1 - \Theta)$, where Θ is the ratio between coverage and maximum coverage), slow diffusion leads to an oxidation behaviour determined by a nucleation and growth mechanism [2–6].

The transition between the high coverage phase and low coverage phase leads to the so-called pre-peak in cyclic voltammetry, which was also observed on polycrystalline Pt and other surfaces (like vicinally stepped Pt(1 1 1) [7–10]),

* Corresponding author. Fax: +49-228-734540.

E-mail address: baltruschat@uni-bonn.de (H. Baltruschat).

¹ Present address: ZSW, Helmholtzstraße 8, D 89081 Ulm, Germany.

and which is often referred to as weakly adsorbed state. By recording potential transients during oxidation of the adsorbed CO under galvanostatic conditions, we were able to show that the oxidation of that amount of CO which desorbs during the transition between the two adsorbate states does not follow any of the Langmuir–Hinshelwood type rate equations [11]. The transients rather suggest an Eley Rideal mechanism. Probably, CO is oxidised at defect sites on the surface, the number of which is constant and to which CO diffuses quickly at high coverages. In contrast, the galvanostatic potential transients during further complete oxidation show the potential maximum typical for both types of Langmuir–Hinshelwood mechanisms (i.e. fast or slow diffusion) only after oxidation of approximately one tenth of the adsorbate at nearly constant potential.

Concerning the action of co-catalysts, there is also an ongoing debate. It is generally accepted that Ru acts according to the bi-functional mechanism, see, e.g. Watanabe and Motoo [12]. On a Pt(1 1 1)-surface covered by 2D Ru islands, CO adsorbed in between on Pt areas is able to diffuse to the Ru sites, where it reacts with oxygen species adsorbed on Ru [13–18]. However, we have recently shown that for very low Ru coverages and large distances between Ru sites CO is oxidised at two different potentials [7]. This has not only been observed in cyclic voltammetry, but has also been verified in galvanostatic potential transients, where two potential plateaus are found [11]. This may either be due to the fact that the diffusion rate depends on CO coverage and is influenced by Ru [7,18] or signify that Ru influences the adsorption enthalpy in its vicinity [11], pointing towards an electronic effect. An argument for the latter assumption is that even the positive of the two peaks is considerably lower than that found on pure Pt. These findings have been substantiated by theoretical calculations [6,19]. It has also been shown that neither of these two effects alone is able to explain the co-catalytic effect of Ru in fuel cell anodes [20].

In the case of less noble co-catalysts, it is also often assumed that they act according to the bi-functional mechanism. In the case of Mo, this effect seems to be limited to the oxidation of the weakly adsorbed CO [21]. In the case of the Pt₃Sn(*hkl*) alloys, a high activity for bulk CO oxidation has been shown that is correlated to a weakly adsorbed state of CO with an onset potential which is lower by approximately 300 mV [22]. Moreover, it was also demonstrated with Sn modifications of Pt single crystal surfaces that a major promoting effect is the shift of the onset potential of the oxidation of the weakly adsorbed state of CO to much lower values and, in addition, that the population of the weakly adsorbed state is drastically increased [7,8,23]. A prerequisite for the high CO oxidation activity of Sn/Pt surfaces is a uniform distribution of co-adsorbed Sn, e.g. by step decoration of the Pt(3 3 2) electrode. The oxidation potential of the “strongly adsorbed state”, on the other hand, is hardly shifted. We therefore assume that contrary to what is generally believed, Sn mainly has an electronic influence on neighbouring Pt atoms, changing the binding energy of

CO to Pt. On a Pt(1 1 1) electrode, Sn is much less active, and this is due to the formation of 2D islands, which, however, are very mobile in the absence of co-adsorbed CO as shown in a recent STM study [24]. For the maximum coverage ϑ (ratio of Sn atoms to surface Pt atoms) of Sn on Pt(1 1 1), we postulated a value of 0.33. This was only based on a correlation of the oxidation peak charge (presumably OH adsorption on or within the Sn adlayer on Pt(1 1 1)) to the suppression of hydrogen adsorption.

It is the aim of this work to get a further insight into the interaction of Sn and CO. CO adsorbed on Sn decorated Pt single crystal surfaces is investigated. The absolute Sn coverage which is of paramount importance for the interpretation of the results was determined by XPS. Furthermore, the structural properties of the electrode surfaces were investigated by studying the influence of co-adsorbed Sn on the vibrational spectra of CO.

2. Experimental

The single crystals were prepared following Clavilier et al.’s flame annealing method [25]. They were about 1 cm in diameter and 3–4 mm thick. After cleaning by cycling in supporting electrolyte they were heated in a hydrogen flame (hydrogen was from Messer Griesheim, purity 5.0) to slightly red colour for 30 s. Afterwards, they were transferred into the electrochemical cell still glowing to cool down in a straight stream of argon (argon was from Messer Griesheim, purity 5.0). This normally takes about 4 min. After this procedure, they were carefully contacted with the electrolyte using the hanging meniscus technique. The preparation was then checked by recording a cyclic voltammogram.

All solutions were made from supra pure sulphuric acid from Merck and suprapure (Millipore) water. The adsorption of tin was performed in a second cell, in order to avoid contamination of the first cell by tin. During the transfers between the two cells a drop of electrolyte protected the surface. Tin solutions were made with 0.5 M H₂SO₄ and Sn SO₄ from Merck; they had to be freshly prepared because of an autocatalytic oxidation of Sn^{II} to Sn^{IV} by oxygen which leads to the build-up of a SnO₂ layer on the glass surface.

Tin was adsorbed at 250 mV for 3 min under potential control. After thoroughly rinsing with ‘Millipore’ water the crystal was transferred back to the tin-free cell. The crystals were cleaned in HNO₃ and fluoric acid after all experiments involving Sn deposition.

2.1. IR measurement

The FTIR spectrometer was a Bruker IFS 66 V with an evacuated chamber to exclude water and CO₂ from the IR beam. The IR light source of the spectrometer is a silicon-carbide spiral (globarTM) and the detector used is a Hg–Cd–Te semiconductor crystal which was cooled with liquid nitrogen.

The measurements were performed in an external reflection geometry and IR absorption experiments with Pt single crystals require a thin-film electrolyte configuration to minimise IR absorption in the aqueous electrolyte. Prior to preparation the crystal was mounted on a special holder, which allows to adjust its height in the cell for normal CVs (“up”) and for IR measurements (“down”; the crystal is located on the CaF₂ window). In the ‘down’ position, the thin layer of electrolytes between the crystal and the window has a thickness of about 3 μm. In ‘up’ position, the electrolyte contact was made in the hanging meniscus configuration, whereas in the position ‘down’ the crystal was fully covered by the electrolyte. In the IR cell, the concentration of sulphuric acid was restricted to 0.1 M H₂SO₄ to prevent dissolution of the CaF₂ window (the solubility of CaF₂ increases with decreasing pH of the solution). CO adsorption was made with the crystal in the ‘up’ position. The potential was held at 50 mV while CO was led over the electrolyte. After 3 min of adsorption argon was bubbled through the electrolyte for 10 min to remove the residual CO.

After positioning the crystal in the “down” position with an orientation of maximum reflection signal, the spectra were recorded at constant potential. Three hundred spectra were averaged for proper signal-to-noise ratio. In the potential range between 50 and 850 mV versus RHE, the spectra were acquired in 100 mV intervals. The spectrum at 850 mV was selected as a reference spectrum and the spectra at lower potentials were normalised with respect to the reference spectrum which was chosen because no CO is adsorbed and no significant oxide is formed at this potential.

For the IR spectra and CVs measurements with lower CO initial coverages the following procedure was applied: 50 μl of a CO saturated solution were injected with a syringe into the IR cell while bubbling with argon and the crystal being in the ‘up’ position at 50 mV. The bubbling was continued for 10 min to remove the residual CO.

2.2. UHV

UHV experiments were carried out in a modified Perkin-Elmer 548 system, which is described in more detail in ref. [21]. The base pressure after bake-out is about 1×10^{-10} Torr and rises up to 3×10^{-9} Torr after a few electrochemical experiments. A gate valve detachable ante chamber with a horizontal moveable glass cell allows to perform the electrochemical experiments without any exposure of the cell to the laboratory ambience. Prior to an experiment the ante chamber was back-filled with highly purified Ar 5.0 to ambient pressure and evacuated to 1×10^{-7} Torr after the experiment.

The disk-shaped Pt(111) single crystal ($\varnothing = 10$ mm, oriented within an accuracy of 0.5°) was attached through two Pt wires to the sample holder. This sample holder allows an hanging meniscus configuration in the electrochemical experiments.

Preparation of the Pt(111) consisted of sputtering (8×10^{-5} Torr Ar 5.0) and subsequent annealing using a custom-built electron-beam gun. Orientation and cleanliness were checked by LEED and AES. A CV (0.5 M H₂SO₄, scan speed 50 mV s⁻¹) was recorded prior to Sn deposition to have additional information on the condition of the surface. As the reference electrode a saturated calomel electrode (with a potential of +0.64 V versus NHE) was used, connected to the working electrode compartment by a Teflon tube. Sn deposition was then carried out by cycling the electrode in a 0.5 M H₂SO₄ solution containing 3×10^{-5} M SnSO₄.

From the XPS data, the coverage of the electrode with Sn (ϑ_{Sn}) was calculated using an internal standard as described in a previous article [21].

3. Results

An absolute value for the coverage of Sn can only be obtained using a spectroscopic method such as XPS. Fig. 1 shows a cyclic voltamogram of Sn-modified Pt(111) recorded in the ante chamber of our UHV system prior to recording the XPS and Auger electron spectra. In the inset of Fig. 1, a CV of the surface in sulphuric acid is shown. We have demonstrated before that the anodic peak at 0.55 V is due to a surface redox process and not due to desorption of Sn [8,24]. An Auger electron spectrum obtained after emersion (Fig. 2) shows that the surface is free from contaminations within the resolution of the measurement. With LEED, only slightly diffuse (1 × 1) spots could be observed.

Fig. 3 shows an example of the XP spectrum. The doublet of the Sn 3d peak, which was used for the quantitative evaluation, is clearly visible. The data are summarised in Table 1. Interestingly, the position of the Sn 3d peak does not depend on the potential at which the electrode is emersed from the electrolyte. The binding energy of 486 eV corresponds to SnO₂. Therefore, Sn is probably oxidised by water after loss of potential control, or, more probably, by sulphate ions staying on the surface, because of its un noble character. Please note that the ratio of the surface concentrations of O to that of S was 4:1 in all experiments. Other origins than sulphate for the oxygen in the SnO₂ would result in higher oxygen coverages (O to S ratio). A similar oxidation by sulphate was suggested for Bi adsorbed on Pt(110) [26].

In order to obtain the coverage which corresponds to full blockage of the hydrogen adsorption, we plotted the hydrogen adsorption charge (as obtained by integration between 0.07 and 0.35 V) versus the coverage as determined by XPS and extrapolated the coverage to full suppression of hydrogen (Fig. 4). This linear extrapolation is justified by the linear relation between residual hydrogen adsorption charge and the charge for the peak at 0.55 V found previously [8,24]. Please note that the charge at zero Sn coverage of 160 μC cm⁻² corresponds to the maximum

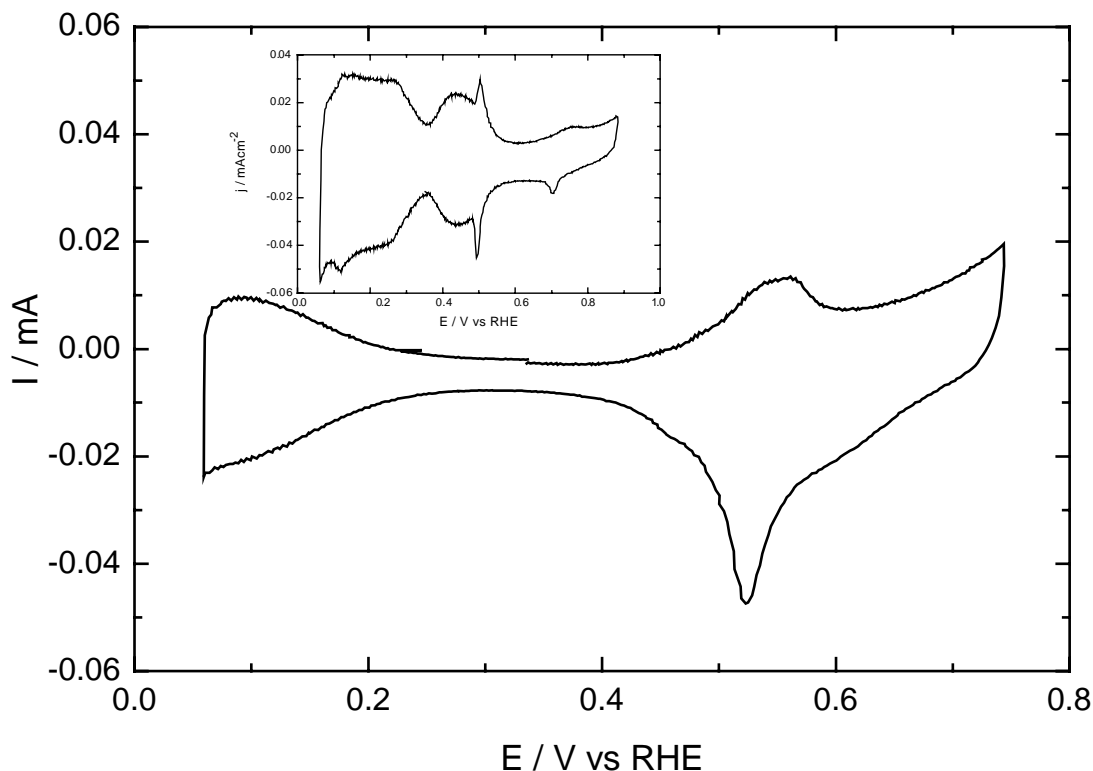


Fig. 1. Cyclic voltammogram (after five cycles) of the Pt(111) (—) in a 0.5 M H_2SO_4 solution containing 3×10^{-5} M SnSO_4 . Scan speed: 50 mV s^{-1} . Inset: For comparison the CV obtained in pure 0.05 M H_2SO_4 in a conventional glass cell is also shown, scan speed 50 mV s^{-1} .

hydrogen adsorption charge at the clean Pt(111). Similar to ref. [24], no background subtraction was used for the data shown in Fig. 4. Since even at the highest achievable Sn coverages a residual limiting charge of $25\text{--}30 \mu\text{C cm}^{-2}$ due to double layer charging is obtained in the hydrogen adsorption region (cf. [8], where in a plot versus the

anodic peak charge a corresponding correction was used for the high Sn coverages), this is the charge corresponding to full blockage of hydrogen adsorption. The value of $\vartheta_{\text{max}} = 0.35$ is, within experimental error, identical to the value of $\vartheta_{\text{max}} = 0.32$ postulated previously. Nevertheless, in the following, all coverage values are given as relative coverages

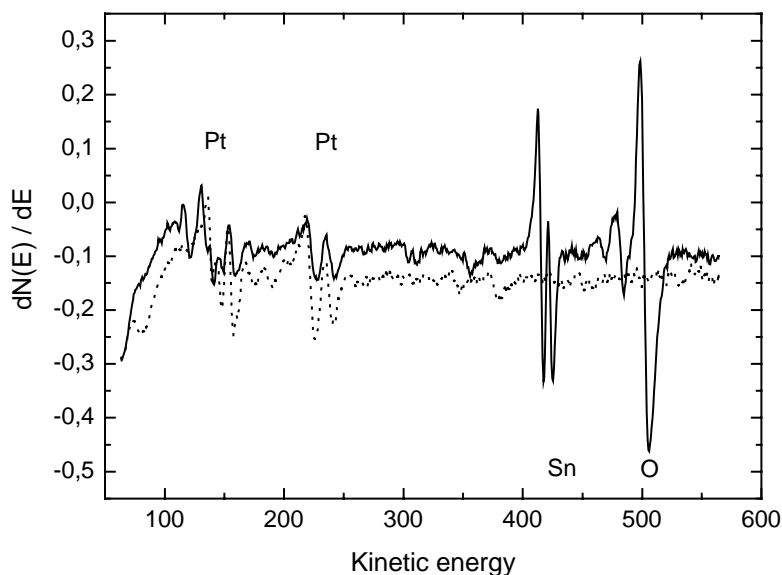


Fig. 2. AES spectrum of the Pt(111) before (---) and after (—) Sn deposition. Prior to the back transfer, the electrode was two times immersed into a 1×10^{-4} M H_2SO_4 solution at $+0.21$ V vs. RHE. $E_{\text{prim}} = 3 \text{ kV}$, $I_{\text{sample}} = 10 \mu\text{A}$.

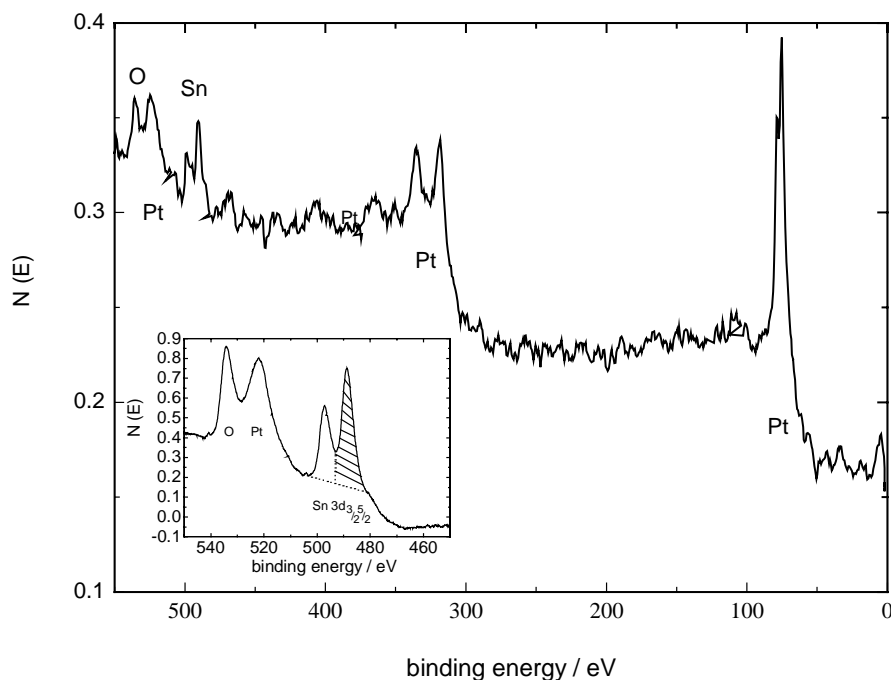


Fig. 3. XPS overview spectra after Sn deposition. *Inset*: Detail showing the Sn 3d_{3/2}, Sn 3d_{5/2} peak, that was used for quantification (hatched area). X-ray power: 14 kV, 14 mA.

as determined from the suppression of the hydrogen adsorption. Absolute coverages are obtained according to Fig. 4, from these using the relation $\vartheta_{\text{Sn}} = 1/3 \times \Theta_{\text{Sn}}^{\text{H}}$.

The influence of UPD-Sn ($\Theta_{\text{Sn}}^{\text{H}} = 0.74$; $\vartheta_{\text{Sn}} = 0.25$) on the IR spectra of co-adsorbed CO on Pt(1 1 1) is shown in

Fig. 5 for different potentials. Spectra for CO on the Sn-free surface are included for comparison and are similar to those reported before [1]. In the latter case, CO occupies three-fold hollow sites (band maximum at 1780 cm⁻¹) at low potential in addition to on-top sites (2067 cm⁻¹). This was ascribed

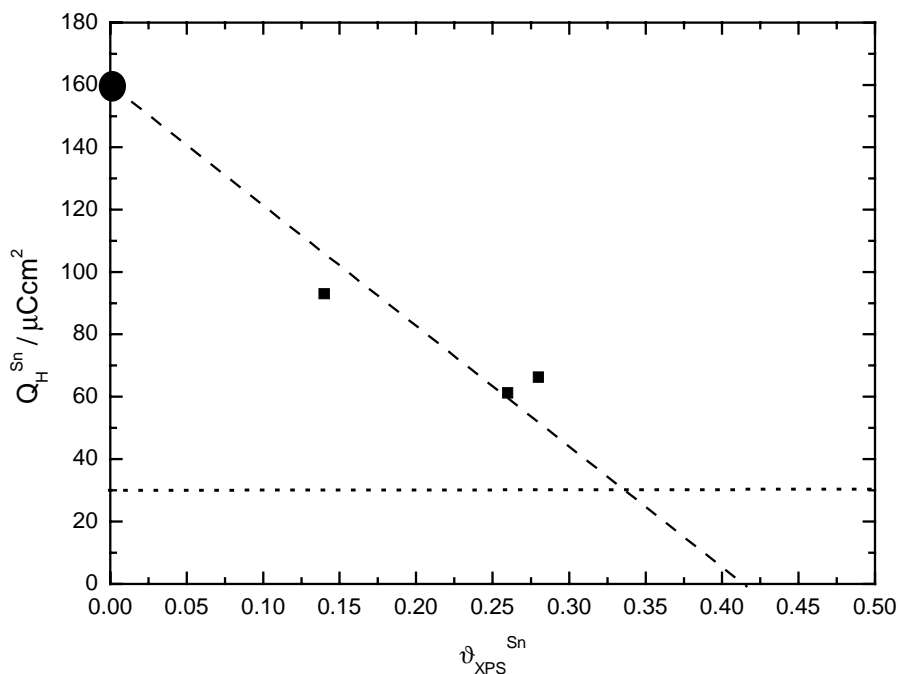


Fig. 4. Plot of the hydrogen charge after Sn deposition Q_{H}^{Sn} obtained from the CV vs. coverage determined by XPS ϑ_{Sn} . The extrapolation is done such that the straight line intersects with the y-axis at 160 μCcm^{-2} . Horizontal line (---): correction of the background charge of the fully Sn-covered Pt(1 1 1), obtained by integration of the CV in the potential range between 70 and 350 mV.

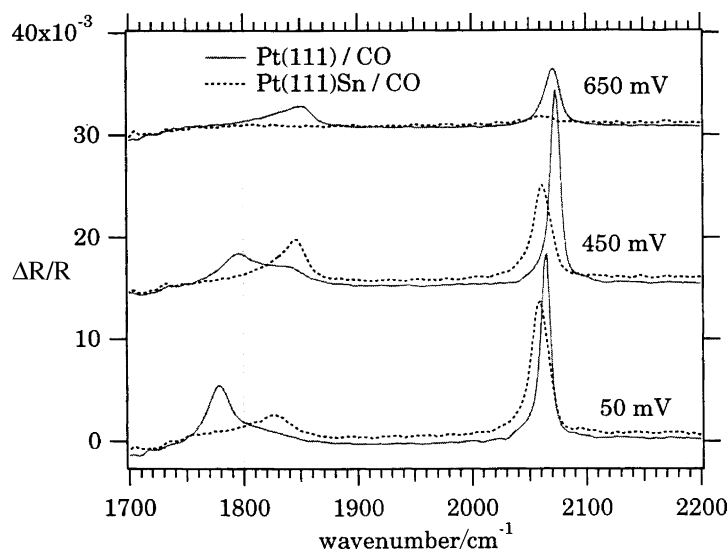


Fig. 5. IR spectra of a saturated CO adlayer on Pt(111) in 0.1 H₂SO₄, with varying potential at $\theta_{\text{Sn}} = 0$ (—) and $\theta_{\text{Sn}} = 0.74$ (---).

to a compressed (2×2) -3CO structure which is transformed into a lower coverage adlayer above 400 mV which was proposed to correspond to a $(\sqrt{19} \times \sqrt{19})R$ 23.4° structure. In the new CO adlayer, CO occupies twofold ($\approx 1840 \text{ cm}^{-1}$) and on-top sites ($\approx 2070 \text{ cm}^{-1}$). The spectrum obtained at 450 mV shows that both structures still coexist at this potential, giving rise to the double peak at 1780 and 1840 cm^{-1} . At 650 mV band, intensities are decreased because oxidation also of the less compressed structure occurs slowly at this potential.

The spectra of the CO stretching vibrations on Sn-modified Pt(111) are best discussed in terms of the band of the system Pt(111)/CO: No additional vibrational bands of CO are present because CO is not adsorbed on tin [27]. However, marked changes compared to Pt(111)/CO are detected when CO is co-adsorbed with Sn. The band signal for CO in threefold hollow sites is negligible even at 50 mV. Interestingly, the spectrum at 50 mV resembles that of CO on the clean Pt(111) surface at 650 mV and the CO layer consists of CO adsorbed in two-fold and on-top sites. Except for changes of the band positions due to the potential dependence of the peak frequency with potential the spectra do not exhibit much variance. One important aspect is the larger band width of the on-top CO band on Sn-modified Pt(111). Values in the range of 15–17 cm^{-1} for the FWHM is found compared to 9–10 cm^{-1} for the neat Pt(111) surface. This is a consequence of inhomogeneous broadening and indicates that the CO adsorbates experience larger variations in their interaction with either the surface or the neighbouring molecules (dipole–dipole interactions). The potential-induced shift in band frequency can be described with equal validity as a change in the of the $d\pi^*$ -CO back-bonding or as a shift due to the static electric field in the double layer, the so-called electrochemical Stark effect. A slight increase of the intensity of the band at 1840 cm^{-1} at 450 mV may be due to the presence

of a small amount of CO adsorbed in hollow sites which are transferred to the bridge site at this potential as on clean Pt(111). Another possible explanation is the increase of the population of the bridge sites due to an expanded adlayer as a consequence of CO electro-oxidation. Note in this respect that the on-top band intensity is decreased significantly. Complete oxidation starts at lower potentials compared to the system without Sn, as seen from the disappearance of the bands at 650 mV.

Spectra for lower Sn coverages ($\theta_{\text{Sn}}^{\text{H}} = 0.2$; $\vartheta_{\text{Sn}} = 0.07$) are shown in Fig. 6 (A and C). When discussing for instance the spectrum at 250 mV it is apparent that all vibrational features discussed before are present. A broad band below 1800 cm^{-1} corresponds to CO in hollow sites and the band above 1800 cm^{-1} is assigned to the bridge site adsorption of CO. In addition, the on-top band shows a shoulder at 2070 cm^{-1} which can be discerned clearly in the spectrum at 250 mV. This frequency coincides with the band position for on-top bonded CO on the Sn-free surface. As a consequence, these spectra can be interpreted as being due to a superposition of spectra for the Sn-free surface and that of the higher Sn-covered surface. Therefore, the most obvious interpretation is that the undisturbed, compressed (2×2) -CO structure (“type I CO”) and an adlayer influenced by tin (“type II CO”) coexists in separate patches on the surface.

The IR-band frequencies for Pt(111) surfaces with different Sn coverages are summarised in Fig. 7. At low potentials, the change of band frequencies with potential (Stark shift) is hardly influenced by Sn and the stretching vibration bands for on-top CO exhibit a potential dependence in the range of about 20 $\text{cm}^{-1} \text{ V}^{-1}$. Furthermore, also the absolute band frequency is only slightly decreased in the case of Sn modifications which is probably due to a reduced dipole–dipole interaction. However, the change of frequency in the potential range of CO oxidation is considerable. This is both due to the start of oxidation at lower potentials as

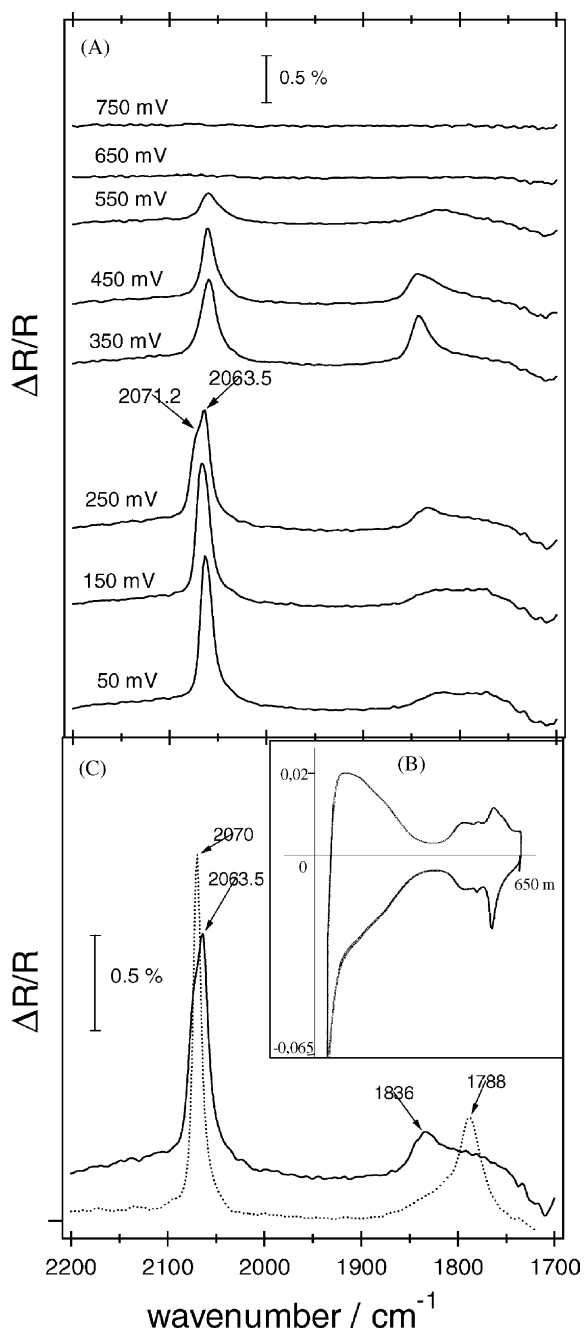


Fig. 6. (A) IR spectra of Pt(111)/ $\theta_{\text{Sn}} = 0.2$ in 0.1 M H_2SO_4 . (B) Cyclic voltammogram in IR cell corresponding to measurements in (A) $dU/dt = 50 \text{ mV s}^{-1}$, $\Delta U = 50\text{--}650 \text{ mV}$ vs. RHE. (C) Comparison of IR spectra of Pt(111) in 0.1 M H_2SO_4 at 0.25 V vs. RHE, $\theta_{\text{Sn}} = 0$ and 0.2.

well as the somewhat increased amount of CO oxidised in the “pre-peak”. The potential dependence of the band frequencies is at variance with a recent publication by Stamenkovic et al. on $\text{Pt}_3\text{Sn}(111)$ electrodes in which a strong Stark tuning slope of $45 \text{ cm}^{-1} \text{ V}^{-1}$ is reported [27]. Also a CO on-top band with frequencies of about 2090 cm^{-1} are shown. This difference is probably related to the distribution of Sn atoms on the surface. Following the interpretation of Stamenkovic et al., the homogenous distribution of Sn in the

alloy electrode leads to a segregation of small CO patches on the surface and to extremely compressed CO islands due to the repulsive interaction of CO and Sn.

4. Discussion

The presence of Sn islands is already obvious from the cyclic voltammogram for the Pt(111) electrode covered by Sn with a coverage $\theta_{\text{Sn}} = 0.07$, shown as insert in Fig. 6(B): The spike at 0.45 V indicates the adsorption of sulphate on Pt(111). If the Sn was distributed homogeneously over the surface no sulphate adsorption current spike would be expected. The Sn islands, however, seem to be very mobile and are only visible by STM when CO is co-adsorbed [24]. For the patches on the surface with type II CO, which is influenced by Sn, there are two possibilities (cf. Fig. 8):

- Either these islands influence CO molecules in their vicinity, giving rise to an adlayer of CO with on-top and bridge site positions; this influence may be electronic in nature, as in the case of Ru [11], or be due to the disturbance of the ordered CO (2×2) adlayer structure close to the islands. Such a disturbance due to steps leading to a disappearance of CO in three-fold hollow sites and appearance of CO in bridge sites was observed in ref. [28,29].
- Or within the islands a mixed adsorbate structure of Sn and CO is formed, similar to that found for the Bi–CO system on Pt(111) [8]. These two possibilities will be discussed below.

Whereas at 50 mV, the bands for both CO adsorbed at three-fold hollow sites and at bridge sites are of equal height, that at 1840 cm^{-1} for bridge site CO starts to increase already at 250 mV. Therefore, the transition of the compressed adlayer to the less compressed one is facilitated by Sn. This is in accordance with the lower oxidation potential of the weakly adsorbed CO on Sn-modified Pt surfaces.

It might be explained by a bi-functional effect of Sn, acting on the oxidation of those CO molecules which are oxidised during the transition from the compressed to the less compressed structure. Since CO does not adsorb on Sn the adsorption of the oxygen species responsible for the oxidation is not hindered by the CO adlayer. We have shown previously, that the main effect of Sn modifying a Pt(111) surface consists in decreasing this onset potential. However, the amount of CO being oxidised in this pre-peak is not largely increased and the potential of the main oxidation peak also is only slightly decreased [8]. Therefore, if Sn acts according to the bi-functional mechanism, it is only active for the weakly adsorbed state (pre-peak). The IR spectra show that not only for type II CO the oxidation potential is decreased. The transfer from three-fold hollow sites to bridge sites rather occurs in that part of the adsorbate which is not in close proximity to Sn and therefore forming

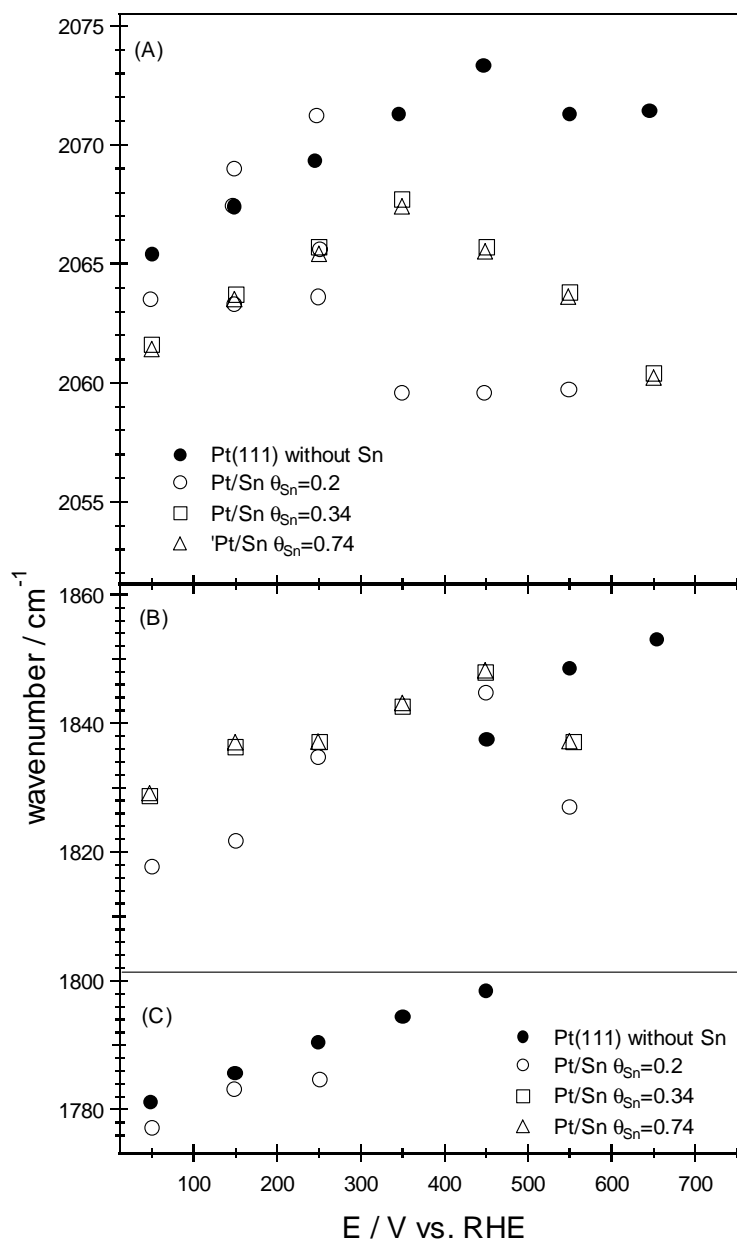


Fig. 7. Wavenumbers of stretching vibrations of CO on Pt(111) for different tin coverages as a function of the oxidation potential. (●) Neat Pt(111)/CO; (○) Pt/Sn $\theta_{\text{Sn}} = 0.2$; (□) Pt/Sn $\theta_{\text{Sn}} = 0.34$; (△) Pt/Sn $\theta_{\text{Sn}} = 0.74$. (A) Potential dependence of band frequencies of on-top CO: at low potentials the on-top stretching band is deconvoluted into two maxima for $\theta_{\text{Sn}} = 0.2$. (B) Potential dependence of band frequencies of bridge-bonded CO: three different tin coverages are compared to neat Pt(111). (C) Potential dependence of band frequencies of the hollow site of CO: three different tin coverages are compared to neat Pt(111).

the compressed layer (type I CO). Probably the repulsive interaction of Sn leads to a lower stable CO coverage on the surface and favouring expanded CO adlayers.

The situation changes drastically when Sn is decorating the steps of a Pt(332) or a Pt(755) surface and forming monoatomic rows: up to 50% of the adsorbed CO is then oxidised in the “pre-peak”. As we have outlined before [8], the only probable explanation for this is, that Sn exerts an electronic, repulsive influence on CO molecules adsorbed in its vicinity. This allows us to distinguish between the two

possibilities mentioned above for the influence of Sn on the IR spectra of type II CO on Pt(111). Is this part of the CO adsorbate influenced by the neighbourhood of pure Sn islands or is it a mixed adsorbate layer with Sn forming islands? It is likely that this part of the adsorbed CO for which the IR spectrum is changed is also the part of the CO which is most easily oxidised due to the action of Sn. The number of molecules thus influenced is larger when, due to step decoration, Sn is forced into a more homogeneous distribution over the surface instead of being adsorbed in

terrace width to 10 rows of Pt atoms [11,30,31]. At a relative Sn coverage of 50%, where CO can adsorb on five rows of Pt atoms, (assuming ideal step decoration, cf. ref. [24]) 60% of CO was found to be oxidised in the pre-peak. Since Sn is adsorbed on both sides of this “band” of Pt, 40% of these Pt atoms are in direct neighbourhood of Sn, meaning that the electronic effect of Sn on Pt only extends over one row of Pt atoms. The pre-peak on Sn covered Pt(1 1 1) is larger than one would expect in this case from the size and distribution of the Sn islands, but this may also be due to the mobility of the Sn atoms when some CO starts being oxidised [24].

We therefore can exclude the formation of a mixed Sn–CO adlattice, but we cannot clearly distinguish between the following two possibilities at this stage:

- (a) An electronic effect of Sn on the Pt atoms in its neighbourhood leads to a higher population of the weakly adsorbed state; the strongly adsorbed state also is present in this electronically modified region.
- (b) The electronic effect of Sn only extends to the next Pt atoms leading to a decreased adsorption energy of CO in very close proximity to Sn.

More experiments using stepped surfaces with a varied terrace size are necessary in order to systematically elucidate the range of the influence of Sn.

In any case, Sn helps considerably in decreasing the CO coverage at low potentials, and therefore enough Pt sites will become available for H₂ oxidation, e.g. in the indirect methanol fuel cell. However, in the case of methanol oxidation (in the direct methanol fuel cell) the coverage of CO formed by oxidative adsorption will not be sufficiently reduced to provide the necessary number of neighbouring Pt sites for methanol oxidation.

5. Conclusion

That coverage of Sn on a Pt(1 1 1) electrode which corresponds to complete suppression of hydrogen adsorption (i.e. $\Theta_{\text{Sn}} = 1$) is $\vartheta_{\text{Sn}} = 0.35$ (Sn atoms per surface Pt atoms), as shown by the XPS results. However, Co-adsorption of CO within this seemingly open adlattice is not possible as already shown by our previous Θ_{Sn} versus ϑ_{CO} relationship.

Sn exerts an electronic influence on CO molecules adsorbed in its neighbourhood. This influence leads to the disappearance of the band at 1780 cm⁻¹ indicative of the (2 × 2)–3CO adlayer at low potentials and to a shift of CO from the strongly adsorbed state to the weakly adsorbed state. Alternatively, the disappearance of the 1780 cm⁻¹ band might also be explained by a disturbed order in the neighbourhood of the Sn islands. Such an effect is observed for CO adsorbed at unmodified stepped surfaces, but it does not lead to a shift to the weakly adsorbed state.

In addition, there also seems to be an effect according to the bi-functional mechanism, which is active only for the weakly adsorbed state but extends over all the surface including that part of the adsorbate, which is not electronically influenced by Sn. Similar to the case of Mo, this effect does not work for the strongly adsorbed CO.

Acknowledgements

Financial support by the DFG is gratefully acknowledged.

References

- [1] I. Villegas, M.J. Weaver, *J. Chem. Phys.* 101 (1994) 1648.
- [2] A.V. Petukhov, *Chem. Phys. Lett.* 277 (1997) 539.
- [3] A.V. Petukhov, W. Akemann, K.A. Friedrich, U. Stimming, *Surf. Sci.* 402–404 (1998) 182.
- [4] M.T.M. Koper, A.P.J. Jansen, R.A.v. Santen, J.J. Lukien, P.A.J. Hilbers, *J. Chem. Phys.* 109 (1998) 6051.
- [5] M.T.M. Koper, A.P.J. Jansen, Lukkien, *J. Electrochim. Acta* 45 (1999) 645–651.
- [6] M.T.M. Koper, J.J. Lukien, A.P.J. Jansen, R.A.v. Santen, *J. Phys. Chem. B* 103 (1999) 5522.
- [7] H. Massong, H.S. Wang, G. Samjeské, H. Baltruschat, *Electrochim. Acta* 46 (2000) 701.
- [8] H. Massong, S. Tillmann, T. Langkau, E.A. Abd El Meguid, H. Baltruschat, *Electrochim. Acta* 44 (1998) 1379.
- [9] N.P. Lebedeva, M.T.M. Koper, J.M. Feliu, R.A. van Santen, *J. Phys. Chem. B* 106 (2002) 12938.
- [10] N.P. Lebedeva, M.T.M. Koper, E. Herrero, J.M. Feliu, R.A. van Santen, *J. Electroanal. Chem.* 487 (2000) 37.
- [11] G. Samjeské, X.-Y. Xiao, H. Baltruschat, *Langmuir* 18 (2002) 4659.
- [12] M. Watanabe, S. Motoo, *J. Electroanal. Chem.* 60 (1975) 275.
- [13] K.A. Friedrich, K.-P. Geysers, F. Henglein, A. Marmann, U. Stimming, W.U. Unkauf, R. Vogel, in: A. Wieckowski, K. Itaya (Eds.), *Electrochemical Society Proceedings*, vol. 96-8, 1996, p. 119.
- [14] W. Chrzanowski, A. Wieckowski, *Langmuir* 13 (1997) 5974.
- [15] K.A. Friedrich, K.P. Geysers, U. Linke, U. Stimming, J. Stumper, *J. Electroanal. Chem.* 402 (1996) 123.
- [16] K.A. Friedrich, K.-P. Geysers, A. Marmann, U. Stimming, R. Vogel, *Z. Phys. Chem.* 208 (1999) 137.
- [17] E. Herrero, J.M. Feliu, A. Wieckowski, *Langmuir* 15 (1999) 4944.
- [18] K.A. Friedrich, K.P. Geysers, A.J. Dickinson, U. Stimming, *J. Electroanal. Chem.* 524 (2002) 261.
- [19] M.T.M. Koper, T.E. Shubina, R.A. van Santen, *J. Phys. Chem. B* 106 (2002) 686.
- [20] P. Liu, J.K. Nørskov, *Fuel Cells* 1 (2001) 192.
- [21] G. Samjeské, H. Wang, T. Löffler, H. Baltruschat, *Electrochim. Acta* 47 (2002) 3681.
- [22] K. Wang, H.A. Gasteiger, N.A. Markovic, P.N. Ross Jr., *Electrochim. Acta* 41 (1996) 2587.
- [23] P. Berenz, S. Tillmann, H. Massong, H. Baltruschat, *Electrochim. Acta* 43 (1998) 3035.
- [24] X. Xiao, S. Tillmann, H. Baltruschat, *Phys. Chem. Chem. Phys.* 4 (2002) 4044.
- [25] J. Clavilier, R. Faure, G. Guinet, R. Durand, *J. Electroanal. Chem.* 107 (1980) 205.
- [26] B.E. Hayden, A.J. Murray, R. Parsons, D.J. Pegg, *J. Electroanal. Chem.* 409 (1996) 51.

- [27] V.R. Stamenkovic, M. Arenz, C.A. Lucas, M.E. Gallagher, P.N. Ross, N.M. Markovic, *J. Am. Chem. Soc.* 125 (2003) 2736.
- [28] A. Rodes, R. Gomez, J.M. Feliu, M. Weaver, *J. Langmuir* 16 (2000) 811.
- [29] S. Tillmann, Zinn-UPD auf Pt(1 1 1), Pt(3 3 2) und Pt(7 5 5), Elektrochemische und IR-spektroskopische Untersuchung des Einflusses auf die CO-Adsorption und Oxidation, Ph.D. Thesis, University of Bonn, Bonn, 1999.
- [30] B. Lang, R.W. Joyner, G.A. Somorjai, *Surf. Sci.* 30 (1972) 440.
- [31] E. Herrero, J.M. Orts, A. Aldaz, J.M. Feliu, *Surf. Sci.* 440 (1999) 259.